A Simplified Approach to Simulate Quench Development in a Superconducting Magnet

Marvin Janitschke, Matthias Mentink, Federica Murgia, Dimitri Pracht, Emmanuele Ravaioli, and Arjan P. Verweij

***Abstract*—Cross-sectional 2D models often represent a computationally efficient alternative to full 3D models, when simulating complex multi-physical magnet systems. However, especially for the case of self-protected, superconducting magnets, where the stored energy has to be dissipated within the magnet coils, the thermal diffusion and the quench development in all three dimensions become key aspects. In order to further improve the simulation of transients in 2D models, a new modelling method for simplified quench development along the direction of the transport current is introduced. The original 2D model is hereby utilized for modelling the thermal domain, and the electrical resistance of each turn is scaled by the estimated time-dependent fraction of quenched conductor. Furthermore, the turn to turn quench propagation following the electrical connections is implemented. The proposed approach allows a very computationally efficient and easy-to-implement calculation since the model is effectively two-dimensional while providing a good approximation of the coil resistance development with sufficient accuracy. In order to illustrate the proposed quench-propagation modelling approach, simulations are compared to experimental results for the case of a self-protected, superconducting Nb-Ti dipole magnet. In general, a very good agreement between measurements and simulations was achieved.**

***Index Terms*—Quench propagation, quench protection, self-protected, superconducting coil, accelerator magnet.**

I. Introduction

SUPERCONDUCTING wires can experience a phenomenon called quench, where parts of the conductor suddenly pass from the superconducting state into the normal state [1]. The resistivity of the superconducting material is rising above the resistivity of the surrounding stabilizer matrix, which then carries the current. The heat generated by ohmic loss diffuses from the initial quench area through the conductor-insulation into the whole coil, leading to a quench propagation inside the magnet. The stored energy of the magnet is dissipated after the quench detection and magnet power source disconnection in the coil winding pack as ohmic and transitory losses [2].

Some types of superconducting magnets do not have an active quench protection system to safely extract the internally stored energy during a transient following a quench. Such magnets fully rely on the mentioned heat propagation to properly dissipate the energy within the coil [3]. Thus, the thermal diffusion and quench development inside the coils are of special interest and the electro-thermal-magnetic model needs to properly take them into account. This challenging problem of quench propagation has been extensively studied in numerous ways using analytical and numerical approaches in one-, two- and three-dimensional models with differing assumptions [4]–[12]. Usually, 2D cross-sectional models are significantly more computationally efficient, compared to complex, full 3D models, but might lack accuracy since 3D-effects are not included.

Further improvements of a purely 2D cross-sectional model of a superconducting magnet for the simulation of transients can be achieved by including an approximated quench propagation into the third dimension. In the proposed approach, the electrical resistance of each turn, following a quench, is multiplied by the estimated time-dependent fraction of quenched conductor in the longitudinal direction, simulating the longitudinal quench propagation as a running wave along the direction perpendicular to the cross-section. The initial quench is thus propagating with an analytically calculated velocity, simplified under some assumptions and spreading throughout the entire magnet coil.

Furthermore, enabling the heat to also diffuse through the magnet wedges separating the coil blocks from each other, as well as including transitory loss between the filaments of the wires, referred to as inter-filament coupling loss (IFCL) [1], [13], [14], and simulating the thermal connection of the outer magnet wires to a thermal sink, additionally improve the accuracy of the 2D thermal model.

The transversal heat diffusion through conductor insulation layers and coil wedges and the longitudinal quench propagation into the consecutive electrically-connected turn are illustrated in Fig. 1.

The proposed technique is implemented using the recently developed program to simulate electromagnetic and thermal transients in superconducting magnets, called STEAM-LEDET (Lumped-Element Dynamic Electro-Thermal) [15], [16], and is compared to experimental results from one self-protected superconducting magnet installed in the CERN Large Hadron Collider (LHC).

Manuscript received November 26, 2020; revised January 17, 2021; accepted February 12, 2021. Date of publication February 17, 2021; date of current version March 12, 2021. *(Corresponding author: Dimitri Pracht.)*

Marvin Janitschke is with CERN, CH, 1211 Meyrin, Switzerland, and also with the Technische Universität Berlin, DE, 10623 Berlin, Germany (e-mail: marvin.janitschke@cern.ch).

Matthias Mentink, Emmanuele Ravaioli, and Arjan P. Verweij are with CERN, CH, 1211 Meyrin, Switzerland.

Federica Murgia was with CERN, CH, 1211 Meyrin, Switzerland. She is now with University of Bologna, 40126 Bologna, Italy.

Dimitri Pracht was with CERN, CH, 1211 Meyrin, Switzerland. He is now with the CHochschule Hannover, DE, 120, 30459 Hannover, Germany.

Color versions of one or more figures in this article are available at https://doi.org/10.1109/TASC.2021.3059980.

Digital Object Identifier 10.1109/TASC.2021.3059980

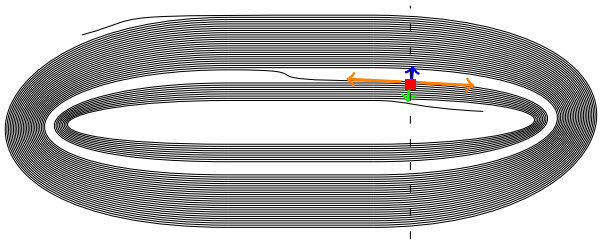

Fig. 1. Coil segment of a superconducting magnet, illustrating the heat diffusion through conductor insulation (green arrow), through coil wedges (blue arrow) and the longitudinal quench propagation along the electrical connections (orange arrows) from the quench origin (red square), 2D cross-section in STEAM-LEDET shown by black, dashed line.

II. 2D Thermal Model and Longitudinal Quench Propagation

The LEDET model features a simplified electrical magnet circuit, a 2D thermal model including ohmic loss, thermal transients between conductors, and a network reproducing coupling effects and loss between the coil and inter-filament current loops in its conductors. The three domains are coupled via equivalent lumped-element sub-networks. The resulting differential equations are solved using the finite difference method with an explicit Euler implementation [16], [17].

The simplified representation of the magnet's electric circuit consists of a power supply, a crowbar, designed to safely carry the circuit current after the power supply is switched off, warm leads resistances, as well as the magnet's inductance and coil resistance.

The thermal sub-network consists of heat-capacitance elements, storing some of the generated heat and exchanging it with others. Energy is introduced to the thermal magnet model in two ways, either via the ohmic loss in a conductor or via coupling loss. The thermal energy is then either exchanged between coil turns or is transferred to other structural magnet components. The thermal balance of one thermal element reads [16]

$$P_{\mathrm{Ohm}} + P_{\mathrm{cc}} + P_{\mathrm{ex}} + P_{\mathrm{Th}} = \overline{c}(T)\frac{dT}{dt}, \quad [\mathrm{W}] \tag{1}$$

where P_{Ohm} [W] is the generated power by ohmic loss in the conductor, P_{cc} [W] the power generated by inter-filament coupling currents, P_{ex} [W] the exchanged heat with other elements, P_{Th} [W] the heat transmitted into a thermal sink, $\overline{c}$ [JK^{-1}] the heat capacity of the element, averaged over its cross-section and T [K] its temperature. Each of the used thermal elements includes superconductor, stabilizer and insulation materials.

A. 2D Thermal Diffusion

The LEDET model approximates the thermal domain as a 2D model at the cross-section where the quench occurs. Hence, the thermal diffusion equation is solved numerically only in the directions perpendicular to the transport current [16]. The computationally expensive longitudinal thermal gradient is neglected. All physical properties are assumed to be uniform within the thermal element. We differentiate three different thermal diffusion components:

Heat Diffusion between Turns (TT): The heat transfer between adjacent turns is usually the main thermal diffusion process in a quench discharge.

Heat Diffusion to Coil Wedges (We): The coil wedges, usually made of a highly conducting metal [1], [18], take up some of the heat and provide a path with a lower thermal resistivity between the coil blocks. The heat can be transmitted across the wedge to the neighbouring block, accelerating the quench propagation within the coil.

Heat Diffusion to Thermal Sink (ThS): Superconducting coils are usually in thermal contact with a surrounding mechanical structure [1], [19]. This structure is modelled as a thermal sink with constant temperature. During a thermal transient, some heat diffuses from the coil turns to the structure. This process can reduce the peak coil temperature [20].

B. 1D Longitudinal Quench Propagation (LP)

After a quench in the cross-section, in a 2D model, the full turn length is considered as quenched. However, in reality a quench first only affects a small part of the conductor and propagates from there further on [2], [21]. The newly proposed feature introduces an analytical estimation of the time-dependent fraction of quenched conductor in the longitudinal direction, which scales the electrical resistance of the turn. The value of this fraction increases linearly with the constant normal-zone propagation velocity [21]–[25]

$$v_{\mathrm{z}} = \frac{J}{\overline{c}}\left(\frac{pk}{T_{\mathrm{cs}}/2 + T_{\mathrm{c}}/2 - T}\right)^{1/2}, \left[\frac{\mathrm{m}}{\mathrm{s}}\right] \tag{2}$$

where J [Am^{-2}] is the current density of the insulated conductor, p [m] its perimeter, k [Wm^{-1}K^{-1}] its thermal conductivity and, T_{cs} and T_{c} [K] its current sharing and critical temperature, respectively. Equation 2 approximates the wave front propagation assuming an adiabatic condition.

Furthermore, the initial quench propagates from turn to turn following their electrical connection. Assuming an initial quench in the center of the magnets longitudinal dimension, the electrically connected return line is brought to quench in $t_{\mathrm{Quench}} = \frac{l_{\mathrm{mag}}/2}{v_{\mathrm{z}}}$ [s], where l_{mag} [m] represents the magnetic length.

The main limitations of this approximation are twofold: first, the longitudinal temperature gradient is neglected, resulting in an overestimation of the average resistivity of each turn, which is calculated with the 2D model at the point where the quench started; second, the increase of quench propagation velocity due to pre-heating of the parts of the coil still superconducting is neglected.

C. Inter-Filament Coupling Loss (IFCL)

During a transient in a superconducting magnet, the time-varying magnetic field leads to the generation of an induced field, opposing the applied magnetic field [1], [13], [14]. This field develops because of local coupling currents between superconducting filaments inside the wire matrix and results in respective transitory loss [13], [26].

The approach using lumped elements in LEDET includes these effects with its coupling-current sub-network, which is composed of equivalent inter-filament coupling current

TABLE I
MAIN MAGNET AND CONDUCTOR PARAMETERS OF THE LHC MCBY MAGNET [19] USED IN THE SIMULATIONS

Parameter	Unit	Value
Nominal current, I_{nom}	A	88
Nominal field strength at I_{nom}	T	3.0
Peak field in the conductor at I_{nom}	T	3.2
Operating temperature	K	1.9
Differential inductance at I_{nom}	H	5.27
Maximal stored energy	kJ	12
Number of turns	-	2670
Magnetic length, l_{mag}	m	0.899
RRR	-	100
Conductor insulation thickness	mm	0.03
Wedge and collar insulation thickness	mm	0.2
Cu/SC Ratio	-	4.4

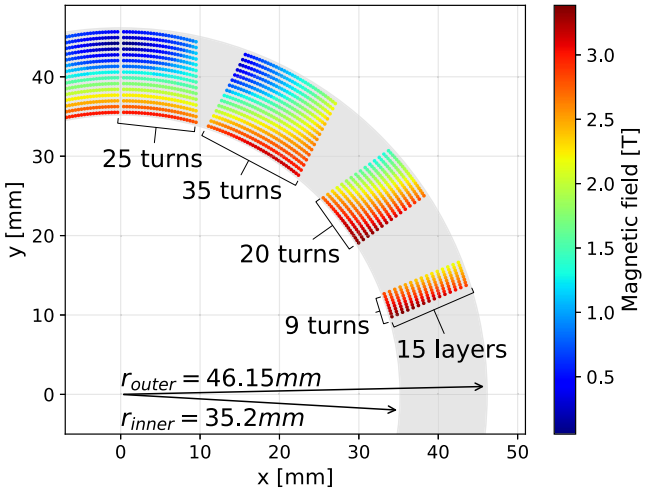

Fig. 2. Magnetic field amplitude in the first quadrant of the LHC MCBY conductor cross-section at nominal current, including the iron yoke effect, calculated using ROXIE [4]. The symmetrical halves of the coils are located in the third and fourth quadrants.

TABLE II
DIFFERENT SIMULATION CASES AND THE INCLUDED MODEL FEATURES, DESCRIBED IN CHAPTER II

Case	TT	We	ThS	LP	IFCL
A	X				
B	X				X
C	X	X	X		
D	X			X	
E	X	X	X	X	X

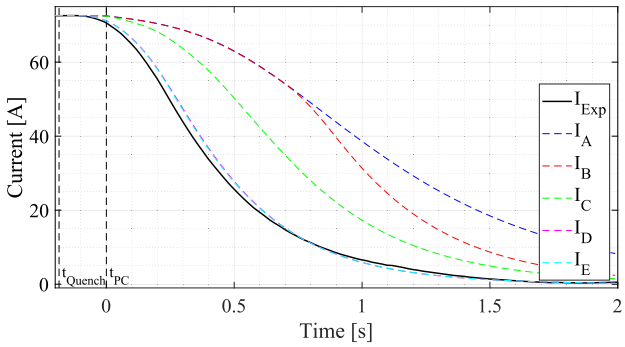

Fig. 3. Simulated current using various model features from STEAM LEDET, compared to experimental current in the MCBY magnet after a quench at $t_{\mathrm{Quench}} = -0.185$ s and power supply switch off at $t_{\mathrm{PC}} = 0$ s.

TABLE III
ERROR BETWEEN MEASUREMENT AND DIFFERENT SIMULATION CASES

Case	RMSE [A]	max($\lvert e \rvert$) [A]	max($\lvert e_{\mathrm{R}} \rvert$) [%]	QL [$10^3 \times \mathrm{A}^2\mathrm{s}$]
A	4.5	39.7	54.8	5.37
B	3.9	39.6	54.6	5.00
C	3.0	34.7	34.1	3.88
D	0.9	3.6	4.9	2.71
E	0.9	3.2	4.4	2.69

loops [16], [27]. The induced loss generates heat within the conductor, which can lead to a quench [13], [17], [20]. Since in first approximation the conductor is uniform along the longitudinal direction, the loss is uniform as well. Persistent currents in the superconducting material are neglected.

III. MODEL VALIDATION

In order to validate the new approach, the simulations are compared to measurements. The magnet used to show the electro-thermal transient is the LHC MCBY magnet [19], a self-protected, superconducting dipole generating a horizontal field and operating at current levels up to 120 A. The magnet and its conductor parameters are shown in Table I. This magnet includes two apertures, which are magnetically decoupled because of the presence of an iron yoke. The magnetic field inside the coil, including iron yoke effects, was calculated using the software ROXIE [4] and is plotted in Fig. 2.

For the validation, the simulations are compared to a transient following a quench. After the quench, occurring at $t_{\mathrm{Quench}} = -0.185$ s, is detected, the power supply is switched off at $t_{\mathrm{PC}} = 0$ s. The internally stored energy is then dissipated in the magnet coil. The circuit includes the resistance of the warm leads $R_{\mathrm{Warm}} = 67$ mΩ and a crowbar $R_{\mathrm{Crowbar}} = 80$ mΩ, both in series to the magnet. There is no active quench protection system. In the simulations, the initial quench hot-spot is assumed in the wire with the highest field in the innermost layer.

The transient measurements are compared to simulations, including different model features, which are shown in Table II. LEDET simulates these with about 4500 time-steps in less than an hour of computation time. In Fig. 3 the discharge of the magnet current following a quench and a fast power abort is shown.

The obtained errors and quench load in the simulation cases are shown in Table III. The errors include the maximum absolute and relative error between experimental I_{Exp} [A] and simulated current I_{Sim} [A] as well as the root mean square error (RMSE). The experimental current and resistance is calculated from the measured output voltage U_{Out} [V] following $I_{\mathrm{Exp}} = \frac{U_{\mathrm{Out}} - U_{\mathrm{Crowbar}}}{R_{\mathrm{Crowbar}}}$ [A], where $U_{\mathrm{Crowbar}} = 0.9$ V represents the voltage drop across the crowbar.

As can be seen by comparing Cases A and B, including the IFCL does not lead to a significant improvement of the simulation accuracy. The coupling effects are not the dominant effect in this transient. The integration of wedges and heat transfer to adjacent coil blocks, as well as thermal diffusion to a thermal sink (Case C), reduce the maximum relative error to about 34%.

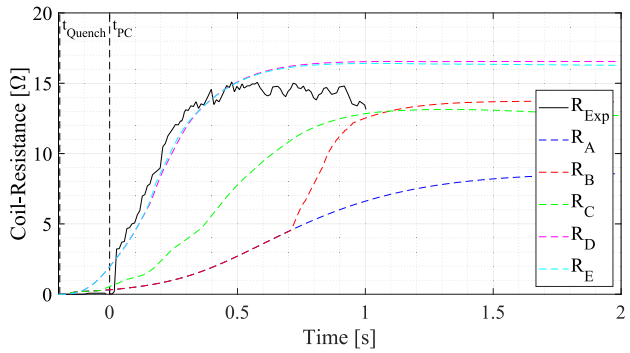

Fig. 4. Simulated coil resistance using various model features from STEAM-LEDET, compared to experimental coil resistance in the MCBY magnet after a quench at $t_{\mathrm{Quench}} = -0.185$ s and a power supply switch off at $t_{\mathrm{PC}} = 0$ s.

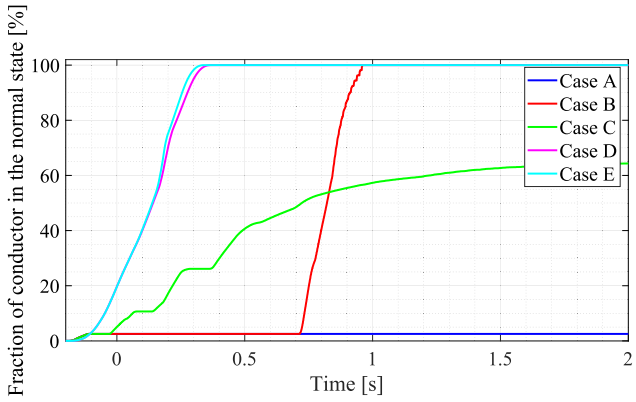

Fig. 5. Simulated fraction of conductor in the normal state for the different cases after a quench in a high-field wire at $t_{\mathrm{Quench}} = -0.185$ s and a power supply switch off at $t_{\mathrm{PC}} = 0$ s.

Simulating the transient with the newly proposed approximation of longitudinal quench propagation (Case D) reduced the error to $<5\%$ and reproduces the transient satisfactorily. Furthermore, including the additional model features into the 2D thermal model (Case E) reduces the error by a further 0.5%. Assuming a quench origin in different high-field spots of the coil can reduce the error further down to $<2.5\%$ or increase it up to 8%.

The quench load (QL) is the time-integral of the squared current. The measured quench load of $\mathrm{QL}_{\mathrm{Meas}} = 2.41 \times 10^3\ \mathrm{A^2 s}$ is reproduced by Cases D and E with an error of about 10%, which correlates to a hot-spot temperature difference of approximately 20 K.

The experimental and simulated coil resistance for the simulations are shown in Fig. 4. The experimental coil resistance was calculated as $R_{\mathrm{Coil}} = \frac{U_{\mathrm{Out}} - L_{\mathrm{mag}}(I)\frac{dI_{\mathrm{Exp}}}{dt}}{I_{\mathrm{Exp}}}$ [Ω], where L_{Mag} [H] is the current-dependent magnet inductance. Due to measurement noise and saturation, the experimental coil resistance is only shown between $t = 0$ s and $t = 1$ s. The coil resistance is defined by the fraction of conductor in the normal state and its temperature. For Cases D and E, the simulated and experimental resistances show good agreement.

The amount of quenched conductor for the simulation cases is shown in Fig. 5. The longitudinal quench propagation, which is modeled with the new feature, leads not only to a normal zone propagation to the adjacent coil blocks but also to the other dipole coil. Not including the feature causes the propagation to be paused after quenching a full coil block. For the analyzed transient, the heat diffusion through the conductor insulation is dominant within a coil block, while the longitudinal quench propagation becomes dominant for the propagation into other blocks. For self-protected magnets, modelling the latter is crucial to accurately reproduce the transient following a quench.

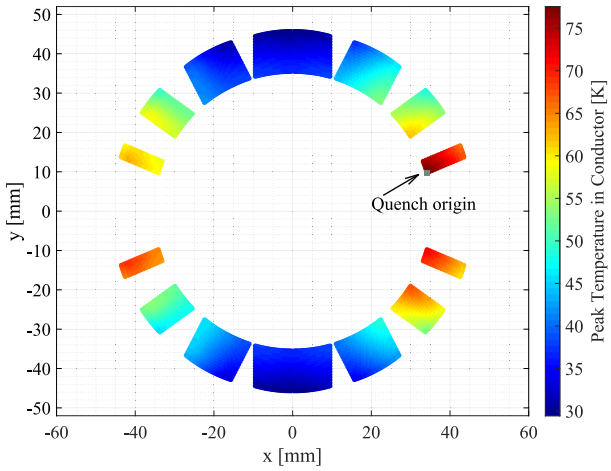

Fig. 6. Simulated peak temperatures of each wire during the transient in the LHC MCBY magnet after a quench at $t_{\mathrm{Quench}} = -0.185$ s and a power supply switch off at $t_{\mathrm{PC}} = 0$ s, including all proposed features (Case E in Table II).

The 2D cross-section of the coil with the peak temperatures for every wire for the simulation including all discussed model features is shown in Fig. 6. The peak temperature obtained during the discharge is below 75 K and is reached in the pole block, where the initial quench started. One can observe that the temperature mostly rises from one corner of a coil block and the radial and azimuthal temperature gradients are similar.

IV. Conclusion

A new feature enhancing 2D cross-sectional electro-thermal quench models was proposed, which approximates the quench development within a superconducting magnet into the third dimension. Therefore, an analytical quench propagation velocity is included, which models the quench propagation along the longitudinal direction throughout the coil. It is shown that including the longitudinal quench propagation and hence allowing the quench to propagate following the electrical connections, can greatly improve the modelling of superconducting magnets.

A quench transient in one self-protected, superconducting LHC magnet was analyzed. Simulations performed with STEAM-LEDET, including different proposed model features, were conducted and validated against measurements. The simulation and measurements show very good agreement. For the case of this self-protected magnet, the newly proposed feature was able to significantly reduce the error of simulations with respect to measurements and opening up the possibility to accurately simulate the electrical and thermal transients.

While the presented LEDET model and its newly proposed additions only represent a 2D cross-sectional model, they are still able to produce a computationally very efficient approximation of the physical quantities with very good accuracy.

REFERENCES

[1] M. Wilson, *Superconducting Magnets, Ser. Monographs on Cryogenics*. Clarendon Press, 1983.

[2] L. Bottura, "Magnet quench 101," *arXiv:1401.3927*, Contribution to WAMSDO 2013: Workshop on Accelerator Magnet, Superconductor, Design and Optimization, CERN, Geneva, Switzerland. [Online]. Available: http://cds.cern.ch/record/1643429

[3] R. Schmidt, C. Giloux, A. Hilaire, A. Ijspeert, F. Rodriguez-Mateos, and F. Sonnemann, "Protection of the superconducting corrector magnets for the LHC," in *Proc. 7th Eur. Part. Accel. Conf.*, Vienna, Austria, Jun. 2000, pp.e-proc, [Online]. Available: https://cds.cern.ch/record/466521?ln=de

[4] S. Russenschuck, *ROXIE : Routine for the Optimization of Magnet X-Sections, Inverse Field Calculation and Coil End Design*. CERN Geneva, 1999.

[5] M. N. Wilson, "Computer simulation of the quenching of a superconducting magnet," RHEL/M 151, vol. 1968.

[6] L. Rossi and M. Sorbi, "QLASA: A computer code for quench simulation in adiabatic multicoil superconducting windings," 2004. [Online]. Available: https://doi.org/10.15161/oar.it/1448979849.04

[7] D. Hagedorn and F. Rodriguez-Mateos, "Modelling of the quenching process in complex superconducting magnet systems," *IEEE Trans. Magn.* vol. 28, no. 1, pp. 366–369, Jan. 1992

[8] F. Sonnemann and M. Calvi, "Quench simulation studies: program documentation of SPQR simulation program for quench research," 2001. [Online]. Available: https://cds.cern.ch/record/691788/files/project-note-265.pdf

[9] G. J. C. Aird, J. Simkin, S. C. Taylor, C. W. Trowbridge, and E. Xu, "Coupled transient thermal and electromagnetic finite element simulation of quench in superconducting magnets," in *Proc. ICAP*, 2006. [Online]. Available: https://accelconf.web.cern.ch/icap06/PAPERS/MOAPMP01.PDF

[10] S. Caspi *et al.*, "Calculating quench propagation with ANSYS," *IEEE Trans. Appl. Supercond.*, vol. 13, no. 2, pp. 1714–1717, Jun. 2003.

[11] P. J. Masson and V. R. Rouault, "Development of quench propagation models for coated conductors," *IEEE Trans. Appl. Supercond.*, vol. 18, no. 2, pp. 1321–1324, Jun. 2008.

[12] L. Bortot *et al.*, "A 2-D finite-element model for electrothermal transients in accelerator magnets," *IEEE Trans. Magn.* vol. 54, no. 3, Mar. 2018, Art. no. 7000404.

[13] A. P. Verweij, "Electrodynamics of superconducting cables in accelerator magnets," Ph.D. dissertation, T.U. Twente, 1995. [Online]. Available: https://cds.cern.ch/record/292595

[14] G. H. Morgan, "Theoretical behavior of twisted multicore superconducting wire in a time-varying uniform magnetic field," *J. Appl. Phys.*, vol. 41, no. 9, pp. 3673–3679, 1970.

[15] "STEAM website," [Online]. Available: https://espace.cern.ch/steam/

[16] E. Ravaioli, B. Auchmann, M. Maciejewski, H. ten Kate, and A. Verweij, "Lumped-element dynamic electro-thermal model of a superconducting magnet," *Cryogenics*, vol. 80, pp. 346–356, 2016.

[17] E. Ravaioli, "CLIQ," Ph.D. dissertation, Enschede, 2015, Jun. 2015. [Online]. Available: http://doc.utwente.nl/96069/

[18] L. Dresner, *Stability of Superconductors. Selected Topics in Superconductivity*. Boston, MA, USA: Springer, 1995.

[19] O. Brüning *et al.*, *LHC Des. Report.* Geneva: CERN, 2004. [Online]. Available: https://cds.cern.ch/record/782076

[20] F. Sonnemann and R. Schmidt, "Quench simulations for superconducting elements in the LHC accelerator," *Cryogenics*, vol. 40, no. 8-10, pp. 519–529, 2000.

[21] H. ten Kate, H. Boschman, and L. Van de Klundert, "Longitudinal propagation velocity of the normal zone in superconducting wires," *IEEE Trans. Magn.*, vol. 23, no. 2, pp. 1557–1560, Mar. 1987.

[22] H. H. J. ten Kate, "Superconducting magnets quench propagation and protection," 2013. [Online]. Available: https://indico.cern.ch/event/194284/contributions/1472819/attachments/281522/393603/TenKate_-_CAS_-Handout-Quench-Erice-2103.pdf

[23] D. Pracht, "Multiphysics modelling of the LHC main quadrupole superconducting circuit," Master Thesis, University of Hannover, 2019. [Online]. Available: http://cds.cern.ch/record/2681097?ln=en

[24] L. Dresner, J. R. Miller, and G. W. Donaldson, "Propagation of normal zones in composite superconductors," *IEEE 6th Symp. Eng. Problems Fusion Res.*, Nov. 1975.

[25] G. Volpini, Ed., *Quench Propagation in 1-D and 2-D Models of High Current Superconductors*, 2009. [Online]. Available: https://www.comsol.com/paper/download/45768/Volpini.pdf

[26] M. Walker, W. Carr, and J. Murphy, "Loss behavior in twisted filamentary superconductors," *IEEE Trans. Magn.*, vol. 11, no. 5, pp. 1475–1477, Sep. 1975.

[27] E. Ravaioli *et al.*, "Modeling of inter-filament coupling currents and their effect on magnet quench protection," *IEEE Trans. Appl. Supercond.*, vol. 27, no. 4, pp. 1–8, Jun. 2017, Art. no. 4000508.